Biomedicine & Pharmacotherapy 143 (2021) 112121

Contents lists available at ScienceDirect

Biomedicine & Pharmacotherapy

journal homepage: www.elsevier.com/locate/biopha

Curcumin analogue C66 attenuates obesity-induced myocardial injury by inhibiting JNK-mediated inflammation

Lin Ye [a,b], Xiaojun Chen [a], Minxiu Wang [a], Leiming Jin [a,b], Zaishou Zhuang [c], Daona Yang [c], Xinfu Guan [c], Aleksandr V. Samorodov [d], Valentin N. Pavlov [d], Nipon Chattipakorn [e], Jianpeng Feng [a], Yi Wang [a], Wu Luo [b,*], Guang Liang [a,f,**]

[a] Chemical Biology Research Center, School of Pharmaceutical Sciences, Wenzhou Medical University, Wenzhou, Zhejiang 325035, China
[b] Medical Research Center, the First Affiliated Hospital of Wenzhou Medical University, Wenzhou, Zhejiang 325035, China
[c] The Affiliated Cangnan Hospital, Wenzhou Medical University, Cangnan, Zhejiang 325800, China
[d] Department of Pharmacology, Bashkir State Medical University, Ufa City 450005, Russia
[e] Cardiac Electrophysiology Research and Training Center, Faculty of Medicine, Chiang Mai University, Chiang Mai 50200, Thailand
[f] School of Pharmaceutical Sciences, Hangzhou Medical College, Hangzhou, Zhejiang 311399, China

ARTICLE INFO

Keywords:
Curcumin derivative
C66
Obesity-related cardiomyopathy
Inflammation
JNK

ABSTRACT

Obesity has been recognized as a major risk factor for the development of chronic cardiomyopathy, which is associated with increased cardiac inflammation, fibrosis, and apoptosis. We previously developed an anti-inflammatory compound C66, which prevented inflammatory diabetic complications *via* targeting JNK. In the present study, we have tested the hypothesis that C66 could prevent obesity-induced cardiomyopathy by suppressing JNK-mediated inflammation. High-fat diet (HFD)-induced obesity mouse model and palmitic acid (PA)-challenged H9c2 cells were used to develop inflammatory cardiomyopathy and evaluate the protective effects of C66. Our data demonstrate a protective effect of C66 against obesity-induced cardiac inflammation, cardiac hypertrophy, fibrosis, and dysfunction, overall providing cardio-protection. C66 administration attenuates HFD-induced myocardial inflammation by inhibiting NF-κB and JNK activation in mouse hearts. *In vitro*, C66 prevents PA-induced myocardial injury and apoptosis in H9c2 cells, accompanied with inhibition against PA-induced JNK/NF-κB activation and inflammation. The protective effect of C66 is attributed to its potential to inhibit JNK activation, which led to reduced pro-inflammatory cytokine production and reduced apoptosis in cardiomyocytes both *in vitro* and *in vivo*. In summary, C66 provides significant protection against obesity-induced cardiac dysfunction, mainly by inhibiting JNK activation and JNK-mediated inflammation. Our data indicate that inhibition of JNK is able to provide significant protection against obesity-induced cardiac dysfunction.

1. Introduction

Obesity, a chronic and complex pandemic caused by genetic and environmental factors, is associated with increased mortality, morbidity, accelerated aging and cardiovascular disease (CVD) [1]. The profound clinical burden of obesity-related CVD can be understood by the fact that BMI > 35 kg/m^2 is associated with a 4-fold increased risk of heart failure [2]. CVD is associated with chronic inflammation, and obesity is recognized as a chronic inflammatory condition [3], which is characterized by the presence of lymphocytes and macrophages [4] and a pro-inflammatory state due to increased production of inflammatory mediators such as interleukin-6 (IL-6) and tumor necrosis factor-α (TNF-α) [5]. The obesity-induced inflammation and increased cytokine levels are both associated with the progression of cardiomyopathy [6]. Enhanced cardiomyocyte apoptosis is one of the important outcomes of inflammation in the obese heart, which is reported as the main cause for the loss of contractile tissue leading to adverse remodeling in the heart of humans as well as in animal models [7]. Contribution of inflammatory cytokine was further confirmed by the inhibition of TNF-α, which protected the heart against inflammation, cardiomyocyte apoptosis, and

* Corresponding author.
** Corresponding author at: Chemical Biology Research Center, School of Pharmaceutical Sciences, Wenzhou Medical University, Wenzhou, Zhejiang 325035, China.
E-mail addresses: wuluo@wmu.edu.cn (W. Luo), wzmcliangguang@163.com (G. Liang).

https://doi.org/10.1016/j.biopha.2021.112121
Received 16 June 2021; Received in revised form 16 August 2021; Accepted 24 August 2021
Available online 30 August 2021

fibrosis in experimental cardiomyopathy models [8], which suggests that inhibition of pathways leading to inflammation or cytokine production may provide a therapeutic strategy to treat obesity-related cardiomyopathy.

Obesity-related chronic inflammation and impaired metabolic homeostasis [9] are associated with the uncontrolled activation of stress-activated protein kinases, such as c-Jun N-terminal kinase (JNK) [10]. The JNK signaling pathway regulates inflammatory response, and impaired JNK signaling is also associated with insulin resistance in obese humans, which demonstrates the role of JNK signaling in obesity-related metabolic disorders, including obesity-related CVDs [11]. We have previously reported that JNK signaling is associated with diabetic cardiomyopathy [12]. However, there is no report on the role of pharmacological JNK inhibition for the treatment of obesity-induced cardiac inflammation and heart dysfunction. We have previously demonstrated that a synthetic derivative of curcumin; (2E,6E)-2,6-bis(2-(trifluoromethyl)benzylidene) cyclohexanone or C66, inhibits inflammatory cytokine production in high glucose or lipopolysaccharide-treated macrophages *via* targeting the JNK [13,14]. The current study was designed to investigate whether C66 treatment prevents activation of JNK signaling and protects the heart against obesity-induced myocardial injury. Our data, for the very first time, demonstrate that JNK inhibition by C66 prevents inflammation and apoptosis in the cardiomyocytes and protects the heart against obesity-induced myocardial injury.

2. Materials and methods

2.1. Cell culture and reagents

An embryonic rat heart-derived H9c2 cell line was obtained from the Shanghai Institute of Biochemistry and Cell Biology (Shanghai, China) and cultured in DMEM (Gibco, Eggenstein, Germany Cat. #C11995500BT) containing 4.5 g/L glucose supplemented with 10% heat-inactivated FBS (Gibco, Eggenstein, Germany Cat. #10270-106), 100 U/ml of penicillin, and 100 mg/ml of Streptomycin (New & Molecular Biotech Co, Jiangsu, China) and grown at 37 °C in an atmosphere of 5% CO_2. Bovine serum albumin (BSA; Cat. #A1933), palmitic acid (C16:0) (PA Cat no. #P9767) were obtained from Sigma-Aldrich (St. Louis, MO). 0.0275 g palmitic acid powder were added in 1 ml of 0.1 M sodium hydroxide and heated at 70 ℃ until dissolved. The palmitic acid sodium is then dissolved in PBS solution with BSA at 45 ℃ heating blender and then stored at −20 ℃ for use.

2.2. Animal experiments

Male C57BL/6 mice (8 weeks old, weighing 18–22 g) were obtained from the Animal Center of Wenzhou Medical University. All animal procedures were approved by the Ethics Committee of Wenzhou Medical University Animal Policy and Welfare Committee. Mice were housed in an environmentally controlled room at 22 ± 2.0 ℃ and 50% ± 5% humidity with a 12:12 h light/dark cycle and feed food and water ad libitum. All animal experiments were performed and analyzed by blinded experiments. Treatment groups were assigned in a randomized fashion. Mice were randomly divided into two weight-matched groups: **(1)** Control group with normal blood glucose (Ctrl group, n = 6) or **(2)** a high-fat diet group (HFD, n = 24) for 11 weeks. Six control mice fed with a standard rodent chow. Normal control diet (containing 10 kcal% fat, 20 kcal% protein and 70 kcal% carbohydrate) and HFD (containing 60 kcal% fat, 20 kcal% protein and 20 kcal% carbohydrate) were purchased from Medicience Diets Co. LTD, Yangzhou, China. After 11 weeks, the HFD group mice were randomly divided into four groups. **(i)** HFD induced obesity mice (HFD group, n = 6), treated with vehicle for C66, **(ii)** HFD-induced obesity mice treated with C66-5 mg/kg (HFD + C66-5 mg/kg group, n = 6), **(iii)** HFD-induced obesity mice treated with C66-10 mg/kg (HFD + C66-10 mg/kg group, n = 6), and **(iv)** HFD-induced obesity mice treated with C66-20 mg/kg (HFD + C66-20 mg/kg group, n = 6). HFD mice were treated with C66 by oral administration once two days from 11th week to 18th week. Mice in Control and HFD groups were orally administrated with the vehicle in the same schedule. All mice were killed under anesthesia at the end of 18th week, the final body weight was measured, and the hearts and blood samples were collected.

2.3. Serum lipid levels detection

Serum triglyceride (TG) was determined using commercial kit. Serum total cholesterol (TCH), serum low-density lipoprotein cholesterol (LDL-C) and high-density lipoprotein cholesterol (HDL-C) were determined using commercial kit (Nanjing, Jiancheng, Jiangsu, China).

2.4. Assessment of heart function

Serum creatine kinase MB (CK-MB) was determined using commercial kit (Nanjing, Jiancheng, Jiangsu, China). Serum atrial natriuretic polypeptide (ANP) and serum brain natriuretic peptide (BNP) were determined using commercial kit (Nanjing, Jiancheng, Jiangsu, China). Systolic and diastolic cardiac functions were determined non-invasively by transthoracic echocardiography in anesthetized mice one day before euthanasia. Diastolic function was assessed using pulsed-wave Doppler imaging of the transmitral filling pattern. Ejection fraction (EF%) was calculated from LV end-diastolic volume (LVEDV) and end-systolic volume (LVESD) using the equation of (LVEDV–LVESV)/LVEDV × 100). Fractional shortening (FS) was calculated using the equation (FS% = [(LVIDd–LVIDs)/LVIDd] × 100).

2.5. Reverse transcription and real-time quantitative PCR

Heart tissues (80–100 mg) were homogenized in TRIZOL (Invitrogen, Carlsbad, CA, USA) for extraction of RNA according to each manufacturer's protocol. Both reverse transcription and quantitative PCR were carried out using a PrimeScript™ RT reagent Kit with gDNA Eraser and SYBR premix Ex Taq II (TAKARA). Bio-Rad CFX96 real time system (Bio-Rad, USA) was used for qPCR analysis. The primers were obtained from Invitrogen (Shanghai, China) and the primer sequences are listed in the Supplementary Table S1. The relative amount of target genes was carried out according to the $2^{-\Delta\Delta Ct}$ algorithm.

2.6. Western blot analysis

Tissue lysate homogenates and cell lysate were prepared. In every western blot analysis, the same amount of total protein from each group was separated by 10–12% SDS-PAGE and electro-transferred onto a nitrocellulose membrane (Bio-Rad Laboratory, Hercules, CA). The membrane was blocked for 1 h at room temperature in TBST (Tris-buffered saline with 0.05% Tween 20, pH 7.4) plus 5% non-fat milk, and incubated with primary antibodies overnight at 4 °C. Antibody p-JNK (Cat. #4668S), JNK (Cat. #9252S), F4/80 (Cat. #70076), p-P65 (Cat. #3033), Bcl-2 (Cat. #3498), Bax (Cat. #5023T) and Cleaved caspase-3 (Cat. #9664S) were obtained from Cell Signaling (Danvers, MA). Antibodies against Col-I (Cat. #ab34710), TGF-β (Cat. #ab92486) and IκB-α (Cat. #ab133462) were purchased from Abcam BioTech. Antibody for GAPDH (Cat. #365062), MyHC (Cat no. #376157) and ICAM-1 (Cat. #8439) were purchased from Santa Cruz Biotechnology (Santa Cruz, CA). After three washes with TBST, membranes were incubated with the appropriate secondary antibody (CST) for 2 h at room temperature. The signals were visualized using enhanced chemiluminescence reagents (Bio-Rad, Hercules, CA). Band intensities were quantified using Image J software (NIH, Bethesda, MD).

2.7. Immunohistochemical determination

The fixed heart tissues were cut into segments for dehydration in a

graded alcohol series, cleared with xylene, embedded in paraffin, and sectioned at 5 μm thickness. For immunohistological preparations, paraffin sections were dewaxed, rehydrated in graded alcohol series, subjected to antigen retrieval in 0.01 mol/L citrate buffer (pH 6.0) for 3 min at 98 °C, and placed in 3% hydrogen peroxide in methanol for 30 min at room temperature. After blocking with 5% BSA, these sections were then incubated with primary antibodies against F4/80 and Col-I at 1:300 dilution overnight at 4 °C, followed by incubation with the appropriate secondary antibodies (1:200, Cell Signaling Technology). The reaction was visualized with DAB solution. After counterstaining with hematoxylin, the sections were dehydrated and viewed under the light microscope (200× amplification; Nikon, Japan).

2.8. Histopathology

Fixed heart tissues were embedded in paraffin and sectioned at 5 μm. After dehydration, sections were stained with hematoxylin and eosin (H&E) kit following manufacturer's protocol. The histopathological damage was evaluated and recorded using a light microscope (200 × amplification; Nikon, Tokyo, Japan).

2.9. Sirius red and Masson staining for collagen

The fixed heart tissue were embedded in paraffin and sectioned at 5 μm thick sections. The sections were stained with the collagen-specific stain, picrosirius red and Masson's trichrome to examine collagen accumulation in kidney tissue and heart tissue. The stained sections were recorded using a light microscope (200× amplification; Nikon, Japan). Collagen deposition was quantified with the Image J program (NIH) using a single blinded method.

2.10. Cell apoptosis assay

For cell lines, cell apoptosis was measured using Annexin V-FITC/ PI Apoptosis Detection Kit according to manufacturer's protocol. For tissue, apoptotic cells were measured using TUNEL staining kit. Briefly, the fixed tissue were embedded in paraffin and sectioned at 5 μm thick sections. The dewaxed, and rehydrated sections were stained with the TUNEL staining kit. Then fluorescent images were observed under a confocal laser scanning microscope (200× amplification; Nikon, Japan).

2.11. WGA-FITC staining

The outline of myocardial cells was demarcated by WGA-FTIC staining. Briefly, the fixed tissue were embedded in paraffin and sectioned (5 μm thick). The dewaxed, and rehydrated sections were incubated with WGA-FTIC at 37 ℃ incubation for 30 min. After washing with PBS (pH7.4), nucleus counterstaining was performed with DAPI. Images were obtained using fluorescent microscope (200× amplification; Nikon, Japan).

2.12. Statistical analysis

Statistical analysis was performed with GraphPad Prism v8.0 Software (San Diego, CA, USA). One-way ANOVA followed by multiple comparisons test with Bonferroni correction was employed to analyze the data. The results are expressed as the mean ± SEM and a p-value < 0.05 was considered significant.

3. Results

3.1. C66 attenuates HFD-induced cardiac dysfunction and myocardial hypertrophy

As shown in Table 1 and Supplementary Table S2, the elevated serum levels of TG, LDL and TCH, and increased body weight (BW) in HFD-fed mice were significantly reduced in C66-treated HFD-fed mice. To confirm HFD-induced cardiac dysfunction and evaluate the effect of C66 treatment, echocardiography analysis was utilized. Echocardiographic assessments revealed reduced ejection fraction and fractional shortening, indicating dysfunctional heart and increased ventricular dimensions, thereby myocardial hypertrophy in HFD-fed mice (Fig. 1A, Table 1). C66-treatment appeared to significantly restore cardiac function and reduce the indices of cardiac hypertrophy in HFD-fed mice in a dose-dependent manner (Fig. 1A, Table 1). Histological analysis of H&E-stained heart sections confirmed our echocardiographic findings in HFD with increased muscle mass and significantly increased longitudinal and transverse cardiomyocyte area, further confirming cardiac hypertrophy; these were reduced in C66-treated HFD-fed mice (Fig. 1B and Supplementary Fig. S1A and B). WGA staining further demonstrated increased cross-sectional cardiomyocyte area in HFD-fed mice, which was significantly reduced in C66-treated HFD-fed mice (Fig. 1C and D). Increased the ratio of heart weight to tibia length (HW/TL) further indicated myocardial hypertrophy in HFD-fed mice; however, C66 treatment restored enhanced HW/TL ratio in HFD-fed mice (Fig. 1E). CK-MB-levels, the most used serologic tests for the diagnosis of dysfunctional heart, were in line with echocardiographic and histological findings. The CK-MB level was enhanced and then significantly reduced in HFD-fed and C66-treated HFD-fed mice, respectively (Fig. 1F). These findings were again confirmed by the molecular indicators of pathological hypertrophy, demonstrated by increased circulatory ANP and BNP levels in the HFD-fed mice, which were reduced in C66-treated HFD-fed mice (Fig. 1G and H). Increased ANP and BNP at the transcript levels in the heart of HFD-fed mice were also significantly reduced by C66 treatment (Fig. 1I and J). Taken together, these data indicate that C66-treatment provided protection against HFD-induced cardiac dysfunction and hypertrophy in mice.

Table 1
Biometric and echocardiographic parameters of the experimental mice.

Parameters	Con	HFD	HFD + C66-5	HFD + C66-10	HFD + C66-20 (mg/kg)
FWd(mm)	0.62 ± 0.0163*	0.8 ± 0.02673	0.725 ± 0.016366*	0.7 ± 0.0188*	0.725 ± 0.0163663*
PWd(mm)	0.6125 ± 0.01*	0.7625 ± 0.01830	0.7 ± 0.00001*	0.6875 ± 0.0226*	0.7125 ± 0.012*
IVSd(mm)	0.675 ± 0.0365*	0.775 ± 0.01637	0.7125 ± 0.0125	0.7125 ± 0.0295*	0.7375 ± 0.026521*
FWs(mm)	0.9 ± 0.032733*	1.0625 ± 0.01830	1.0125 ± 0.035038*	0.9625 ± 0.04199*	0.9875 ± 0.035034*
PWs(mm)	0.8875 ± 0.0226*	1 ± 0.01890	0.95 ± 0.026726*	0.95 ± 0.04225*	0.9375 ± 0.026302*
IVSs(mm)	0.9 ± 0.00002*	1.025 ± 0.01637	0.95 ± 0.018898*	0.9625 ± 0.0375*	0.95 ± 0.02672*
LVd(mm)	2.6 ± 0.1133*	2.4625 ± 0.12092	2.725 ± 0.183955*	2.7125 ± 0.127*	2.75 ± 0.113389*
LVs(mm)	1.4375 ± 0.105*	1.5 ± 0.10690	1.6125 ± 0.110901*	1.5625 ± 0.0625*	1.5875 ± 0.061054*
EF%	82.44125 ± 1.63*	76.68125 ± 1.84252	78.2175 ± 1.353155*	79.76125 ± 0.9288*	79.76375 ± 0.652004*
FS%	45.2175 ± 1.7494*	39.48 ± 1.54680	40.8475 ± 1.227661*	42.235 ± 0.94376*	42.1975 ± 0.64650*
BW(g)	26.83 ± 0.73*	50.48 ± 0.69	42.1 ± 0.92*	40.35 ± 2.90*	40.41 ± 1.89*

Transthoracic echocardiography was performed on mice at the ending of the animal study. EF ejection fraction %, FS, fractional shortening %; LVIDd, diastole left ventricle internal dimension; PWd, diastole posterior wall thickness; IVSd, diastole interventricular septal thickness; BW, body weight. Data presented as Mean ± SEM, n = 6 per group. * $p < 0.05$ compared to HFD group.

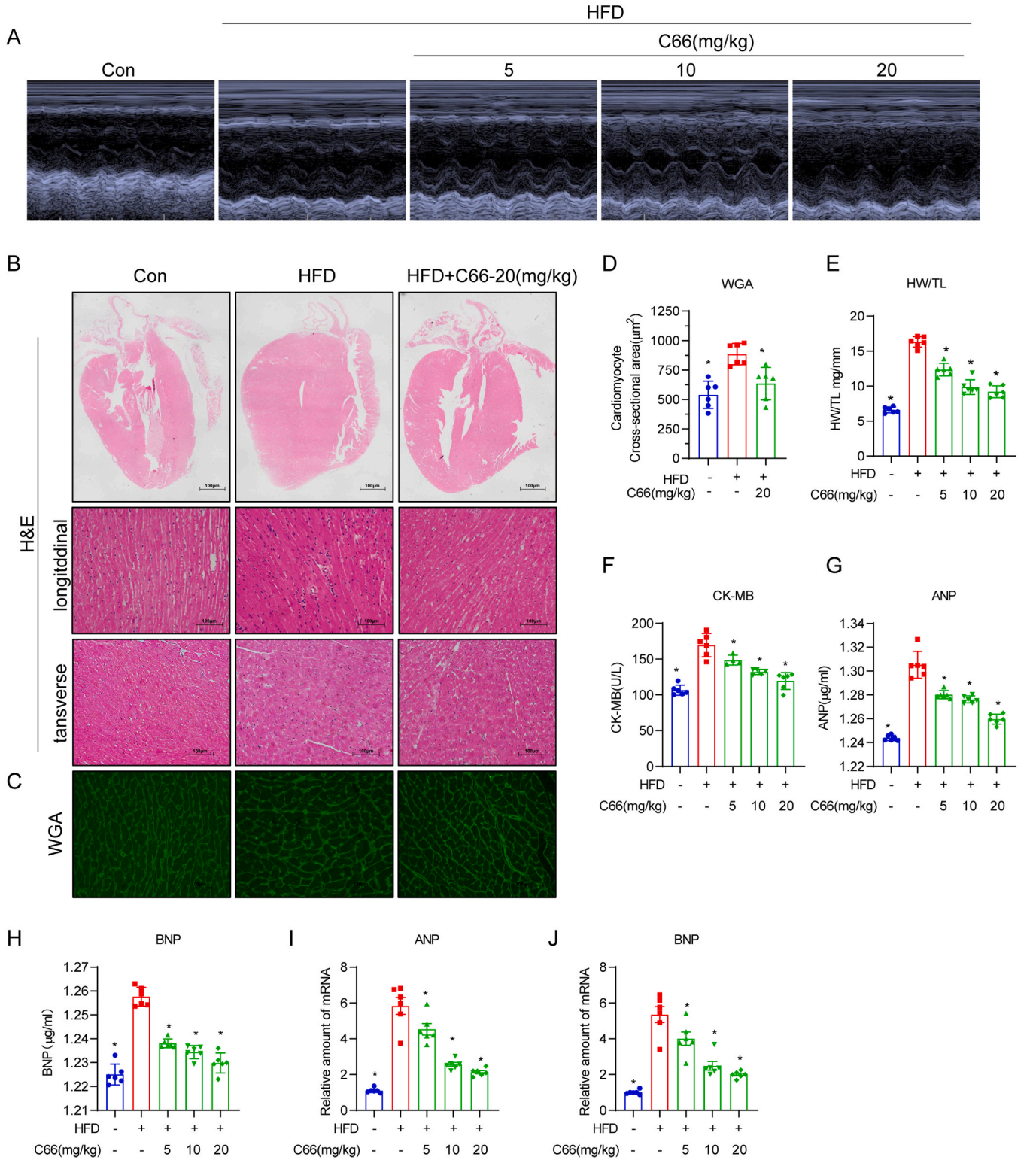

Fig. 1. C66 attenuates HFD-induced cardiac dysfunction and myocardial hypertrophy. Mice were fed with a HFD and infused with either control vehicle or different dose of C66 (5, 10 or 20 mg/kg) 3-times/week for 13 weeks. Later, echocardiography was performed, and heart and serum were collected to perform histology & RNA extraction and biochemical analysis, respectively. (A) Representative echocardiography M-mode images in mice. (B) Representative panoramic (upper), longitudinal (middle), and transverse (lower) images for hematoxylin and eosin (H&E) staining of myocardial tissues (scale bar = 20 μm). (C) Representative images for WGA staining of myocardial tissue and (D) quantification of myocardial cell area (scale bar = 20 μm). (E–H) Bar graphs showing the heart weight to tibia length ratios (HW/TL) (E), circulating levels of Creatinine Kinase-MB (F), atrial natriuretic peptide (ANP) (G), and brain natriuretic peptide (BNP) (H) in mice. Total RNAs were extracted from the heart and qPCR was performed for ANP (I) and BNP (J). Gene β-actin was used for qPCR data normalization. Data are presented as mean ± S.E.M. *P < 0.05, compared to HFD (n = 6 per group).

3.2. C66 administration attenuates HFD-induced myocardial fibrosis and apoptosis

Sirius red and Masson's trichrome staining for total collagen content demonstrated significantly increased collagen deposition, indicating a significantly higher amount of fibrosis in the heart of HFD-fed mice; this was significantly reduced in C66 treated HFD-fed mice (Fig. 2A–D and Supplementary Fig. S2A–C). The deposition of collagen-I (Col-I) was

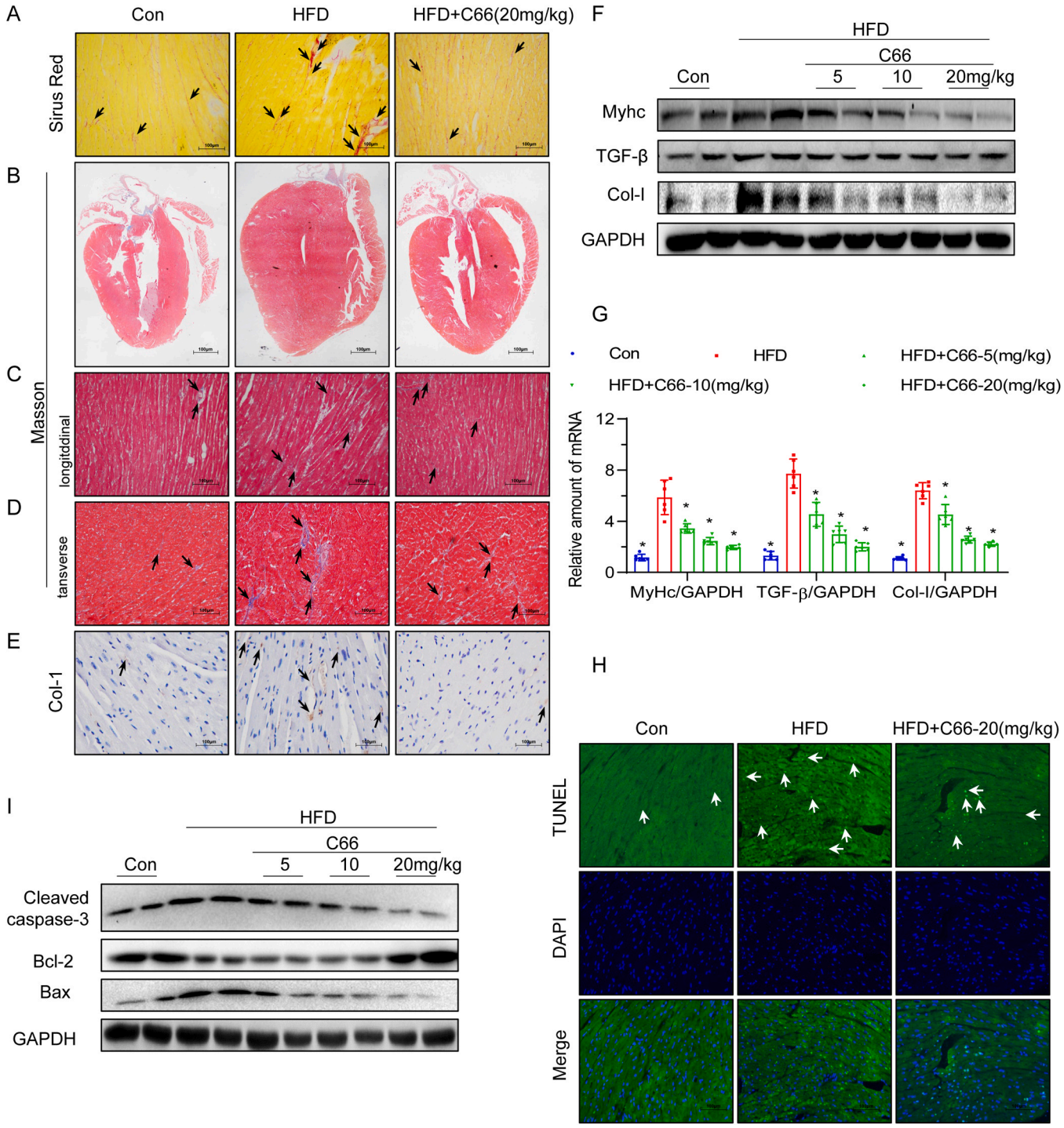

Fig. 2. C66 administration attenuates HFD-induced myocardial fibrosis and apoptosis. Mice were fed with a HFD and infused with either control vehicle or different dose of C66 (5, 10 or 20 mg/kg) 3-times/week for 13 weeks. Later, hearts were collected to perform immunohistology, and RNA and protein were extracted to perform immunoblotting and qPCR, respectively. (A) Representative micrograph demonstrating Sirius red staining of the heart section. (B) Masson's trichrome staining with panoramic (upper), (C) longitudinal (middle), and (D) transverse (lower) sections, (scale bar = 20 μm) and (E) collagen-I (Col-I) staining of the heart sections. (F) Immunoblotting performed on heart proteins for Myhc, TGF-β and Col-I. GAPDH was used as a loading control. (G) Real-time PCR data for Col-IV, TGF-β and MMP-9 on total RNA extracted from the heart. Data normalized to β-actin expression. (H) Representative images for TUNEL staining and quantification of myocardial cell apoptosis (scale bar = 20 μm). Nuclei were stained with DAPI (blue). TUNEL-positive nuclei are indicated by white arrows. (I) Immunoblotting data for cleaved caspase-3, Bax, and Bcl-2. GAPDH was used as a loading control. Data are presented as mean ± S.E.M. n = 6 per group; *P < 0.05, compared to HFD. (For interpretation of the references to color in this figure legend, the reader is referred to the web version of this article.)

evaluated by immunohistochemical analysis, which showed that a significantly increased amount of Col-1 deposition in the heart of HFD-fed mice was inhibited by C66 treatment (Fig. 2E and Supplementary Fig. S2D). Increased Col-I accumulation in the heart of HFD-fed mice was also confirmed at protein and transcript levels *via* immunoblotting and qPCR, respectively, while C66-treatment to the HFD-fed mice reduced the expression level of Col-I in the heart of HFD-fed mice (Fig. 2F and G and Supplementary Fig. S2E). We also measured the expression level of TGF-β and Myhc, which are markers for cardiac fibrosis and hypertrophy, respectively, HFD significantly induced the cardiac expression of TGF-β and Myhc, which was reduced by all the three doses of C66 treatment in a dose-dependent manner at both protein and transcript levels (Fig. 2F and G and Supplementary Fig. S2E). Cardiomyocyte apoptosis plays an important role in the development of obesity-induced cardiomyopathy. Our TUNEL-staining data demonstrate a significantly higher amount of apoptosis in the cardiomyocytes of HFD-fed mice, which was significantly reduced after C66 treatment to the HFD-fed mice (Fig. 2H and Supplementary Fig. S2F). Apoptosis data

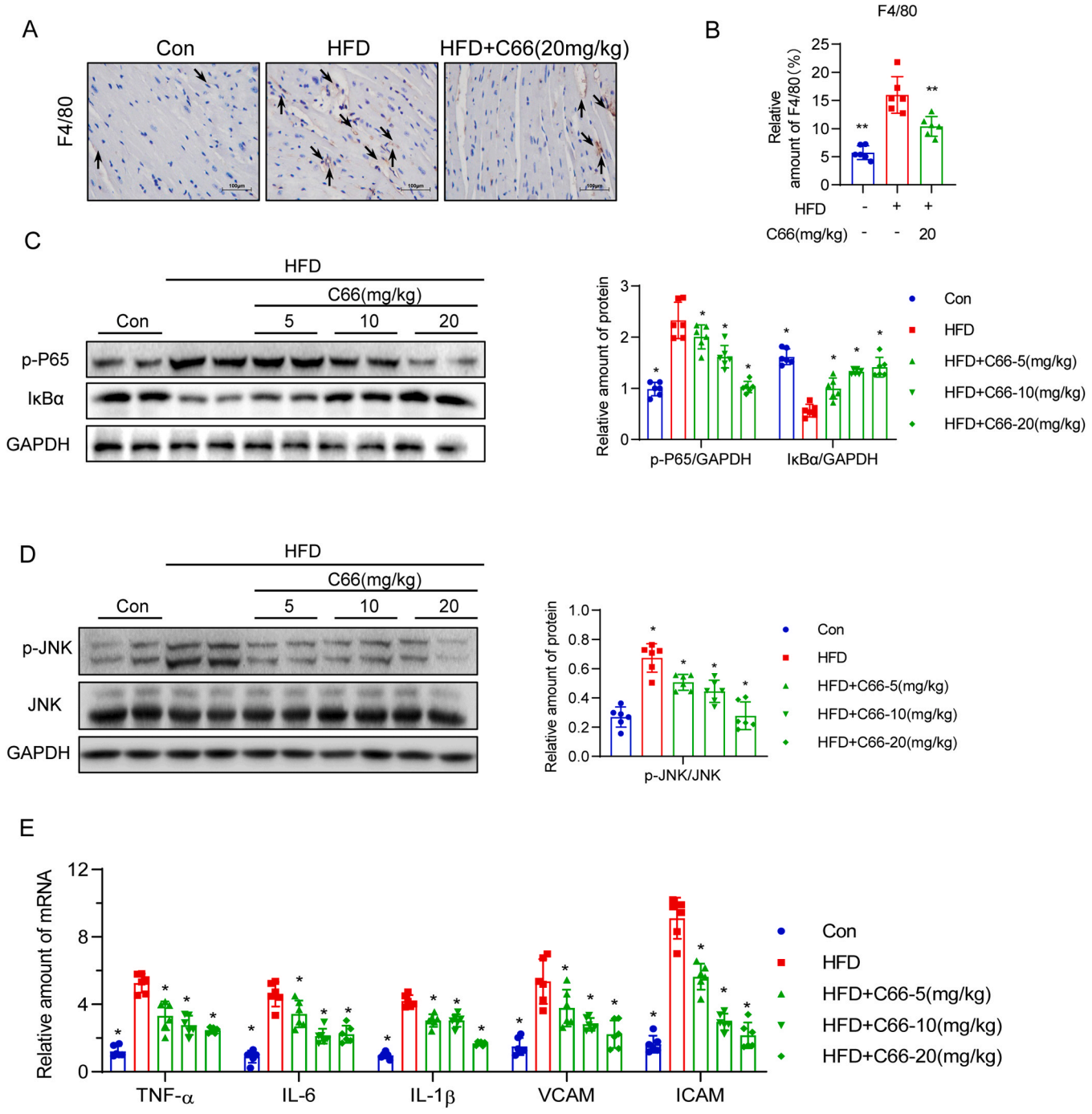

Fig. 3. C66 administration attenuates HFD-induced myocardial inflammation by inhibiting NF-κB and JNK activation. Mice were fed with a HFD and infused with either control vehicle or different dose of C66 (5, 10 or 20 mg/kg) 3-times/week for 13 weeks. Later, hearts were collected to perform immunohistology, and RNA and protein were extracted to perform immunoblotting and qPCR, respectively. (A) Representative image of immunohistochemical staining for macrophage marker (F4/80) and (B) percent quantification of F4/80-positive cells (scale bar = 20 μm). (C) Immunoblotting for p-P65, IκBα, and their quantification. (D) Immunoblotting for p-JNK and JNK, and their ratio quantification. (E) Real-time PCR data for TNF-α, IL-6, IL-1β, VACM, and ICAM. Data normalized to β-actin gene. Data are presented as mean ± S.E.M. n = 6 per group; *P < 0.05, compared to HFD.

were confirmed by immunoblotting for cleaved caspase-3, which showed that increased cleaved caspase-3 in the heart of HFD-fed mice was significantly reduced by C66 (Fig. 2I and Supplementary Fig. S2E). Bax, an accelerator of apoptosis, and Bcl-2, an inhibitor of apoptosis, are the determinants of cardiomyocyte survival and/or apoptosis. Our data demonstrate that HFD significantly increased the level of pro-apoptotic Bax and inhibited the level of anti-apoptotic Bcl-2 in the heart, while C66 treatment reversed these changes, therefore, shifting the overall *milieu* towards cardiomyocyte survival (Fig. 2I and Supplementary Fig. S2F).

3.3. C66 administration attenuates HFD-induced myocardial inflammation by inhibiting NF-κB and JNK activation

The effects of C66 on HFD-induced inflammation in the heart were assessed. Fig. 3A and B shows that HFD induces F4/80-positive macrophage infiltration in the heart of HFD-fed mice, while C66 treatment significantly inhibited the macrophage infiltration. NF-κB mediates inflammation, and HFD is known to activate NF-κB in the heart. We observed an increased NF-κB p65 level and a reduced IκBα level in the heart of HFD-fed mice in comparison to control, indicating increased NF-κB activation (Fig. 3C). However, all three doses of C66 inhibited NF-κB activation in the heart of HFD-fed mice. We next evaluated the activation of JNK signaling in the heart of HFD-fed mice with or without C66 treatment. HFD induced significant phosphorylation of JNK in the heart, while C66-treatment was able to reduce the JNK activation in the heart of HFD-fed mice (Fig. 3D). NF-κB and JNK activation is associated with increased inflammatory cytokine production, such as TNF-α, IL-6, and IL-1β. As expected, we observed a significant increase in the transcript levels of these cytokines in the heart of HFD-fed mice; however, all three doses of C66 successfully prevented the up-regulation of these inflammatory cytokines (Fig. 3E). Heart disease is also known to correlate with the expression of the intercellular adhesion molecule-1 (ICAM-1) and vascular cell adhesion molecule-1 (VCAM-1). As expected, the HFD-induced over-expression of ICAM-1 and VCAM-1 was significantly inhibited by all three doses of C66 treatment (Fig. 3E).

3.4. C66 prevents Palmitic Acid (PA)-induced myocardial injury and apoptosis in H9c2 cells

We first treated cultured H9c2 cardiomyocyte cell line with 200 μM of Palmitic Acid (PA), a dose used by other groups [15], and evaluated for the expression of the hypertrophic and pro-fibrosis genes. As shown in Fig. 4A–C, PA induced significant expression of MyHc, ANP, BNP, TGF-β, Col-1, and MMP-9, at the transcript and protein levels. Pre-treatment of PA-treated H9c2 cells with 2.5, 5 and 10 μM of C66 inhibited the expression of these genes in a dose-dependent manner (Fig. 4A–C). As a positive comparison, JNK inhibitor SP600125 (SP) also showed significant inhibition against these genes in PA-challenged H9c2 cells (Fig. 4A–C). We then evaluated the effect of C66 and SP on PA-induced apoptosis in H9c2 cells. Similar to our *in vivo* finding, significant induction of apoptosis evidenced by immunoblotting for cleaved caspase-3 and Bax/Bcl2 ratio was reversed by C66 or SP treatment in PA-challenged H9c2 cells (Fig. 4B and D). The flow cytometry data confirmed our apoptosis data. PA-induced increase in apoptotic cells was significantly reduced by C66 treatment (Fig. 4E and F).

3.5. C66 inhibits PA-induced JNK/NF-κB activation and inflammation in H9c2 cells

Similar to our *in vivo* observation, C66 treatment was able to reduce PA-induced NF-κB activation; confirmed by reduced p65 phosphorylation and translocation to the nucleus, and by increased IκBα accumulation in H9c2 cells (Fig. 5A and B). C66 treatment also reduced PA-induced JNK activation in H9c2 cells (Fig. 5C). We then assessed the effect of C66 on PA-induced pro-inflammatory cytokine expression in H9c2 cells. C66 treatment was able to significantly reduce the over-expression of these pro-inflammatory genes (TNF-α, IL-6, IL-1β, VCAM-1, and ICAM-1) in a dose-dependent manner (Fig. 5D). Similar to C66, specific JNK inhibitor SP at 10 μM also inhibited PA-induced JNK/NF-κB activation and inflammation in H9c2 cells (Fig. 5A–D).

4. Discussion

Curcumin analog C66, which was developed in our laboratory, exert anti-inflammatory effects both *in vitro* and *in vivo* in several disease models, including models of metabolic disorders such as diabetic complications. The current study demonstrates a protective effect of curcumin analog C66 on obesity-induce cardiac inflammation, hypertrophy, fibrosis, and dysfunction, overall providing cardio-protection against obesity-induced cardiac dysfunction. The protective effect of C66 is attributed to its potential to inhibit JNK activation, which led to reduced pro-inflammatory cytokine production and apoptosis in cardiomyocytes providing cardiac benefit to obese mice.

An increasing number of clinical and animal studies have demonstrated the involvement of the innate immune system and low-grade chronic inflammatory responses in the development of obesity-induced cardiac dysfunction [16]. There are also reports that obesity activates monocytes and macrophage infiltration and induces the expression of pro-inflammatory cytokines and causing inflammation in the heart [5]. There is a dynamic interplay between cardiac fibrosis and inflammation, and these two represent the major pathophysiological mechanisms operating in the failing heart regardless of the etiology of heart failure [17]. Additionally, infiltrated macrophages secrete pro-fibrotic cytokines such as TGF-β, which promotes cardiac fibrosis [18]. We also report that obesity stimulated increased cardiac dysfunction, increased macrophage infiltration, increased pro-inflammatory cytokine production, increased pro-fibrotic molecules and increased apoptosis in the heart, which was significantly reduced by C66 treatment Our *in vitro* data in PA-treated cultured cardiomyocytes also supported *in vivo* data as PA-induced expression of pro-fibrotic molecules and apoptosis both were reduced following C66 treatment.

Increased macrophage infiltration, pro-fibrotic molecules and pro-inflammatory cytokine production *via* NF-κB- or JNK-dependent mechanism is also reported in the failing human hearts [19]. NF-κB activation is known to play roles in the development of cardiac dysfunction [20], and NF-κB inhibition is associated with reduced apoptosis and inflammation in the heart [13,21]. C66-treatment is reported to inhibit NF-κB-dependent inflammation and inflammatory cytokine production [22,23] and additionally, we have shown that C66 inhibits NF-κB and thereby high-glucose induced inflammation [21]. Accordingly, we reported NF-κB activation in the heart of obese mice, which was significantly reduced by C66 treatment in the heart of HFD-fed mice *in vivo* and in PA-treated cardiomyocytes *in vitro*.

Interestingly, we have previously demonstrated that C66 directly interacts with JNK [24] and that C66-treatment inhibits NF-κB signaling and expression of inflammatory cytokines as well as adhesion molecules, such as ICAM1 and VCAM1, by inhibiting JNK signaling *in vitro* and *in vivo* in the kidney of the diabetic animal models [24]. Adhesion molecules play important roles in inducing inflammatory cell infiltration [24–26], and inhibition of ICAM-1 is shown to ameliorate inflammatory cell infiltration and thereby inflammation [24,27,28]. Along with ours, there are other reports indicating that JNK signaling is upstream to NF-κB and can activate NF-κB under stress conditions [24,29,30]. JNK signaling is known to be activated in response to inflammatory and stressful stimuli, such as hyperglycemia *in vivo* or high glucose *in vitro* [30,31]. The JNK signaling also participates in apoptotic pathway initiated by death receptors or TNF-α [32–34], and directly relevant to the present work, JNK activation-mediated cardiomyocyte death is reported in diabetic cardiomyopathy [33,35]. Furthermore, TNF-α can also activate JNK to induce apoptosis [36]. Accordingly, our obesity model was associated with increased JNK activation, VCAM1 & ICAM1

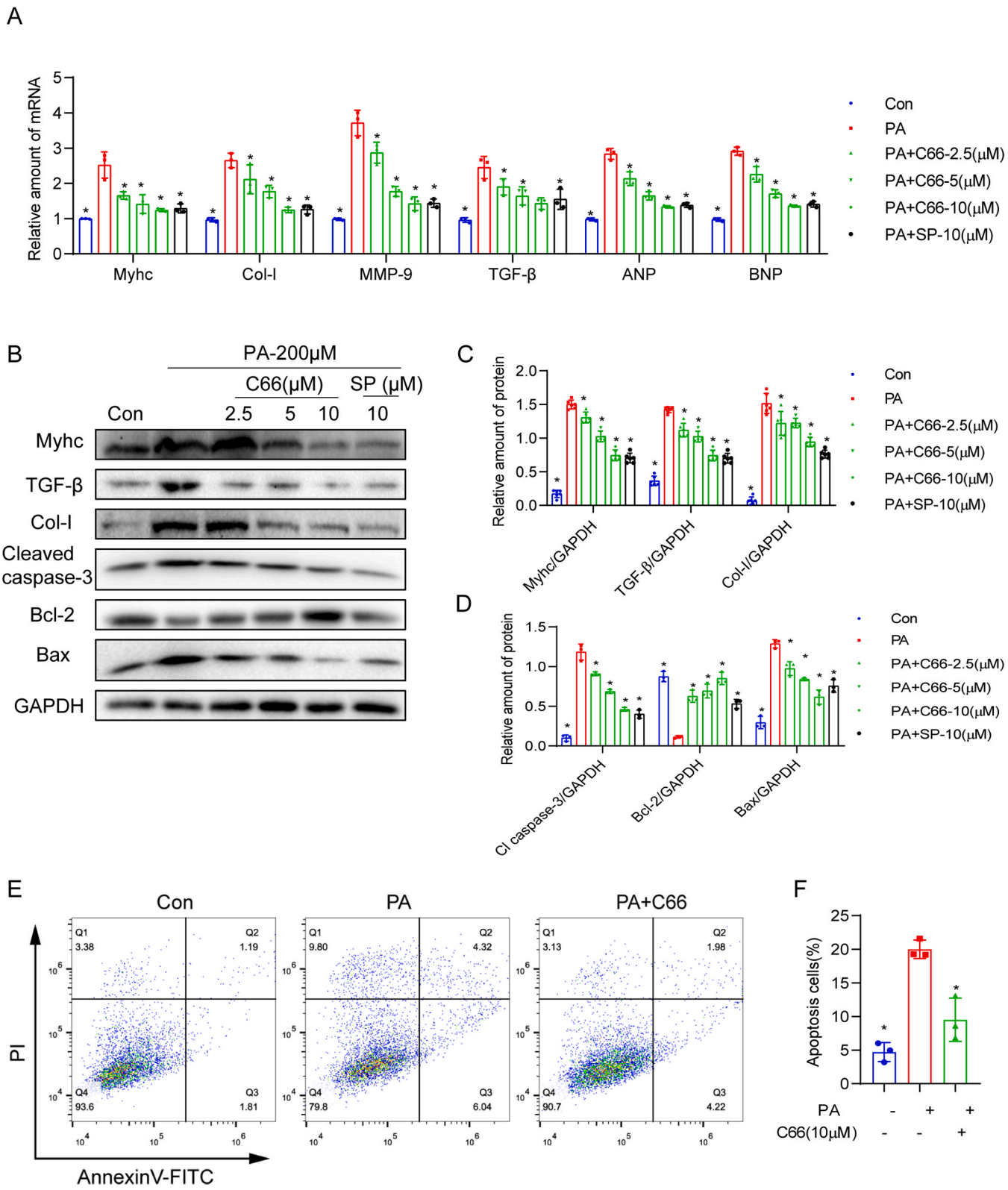

Fig. 4. C66-treatment or JNK inhibition prevents Palmitic Acid (PA)-induced myocardial injury and apoptosis in H9c2 cells. H9c2 cells were pretreated with 2.5, 5, 10 μM of C66 or 10 μM of JNK inhibitor SP600125 for 2 h followed by exposure to PA (200 μM) for 24 h, and then RNA and protein were extracted to perform (A) qPCR for Myhc, Col-I, MMP-9, TGF-β, ANP and BNP. (B) Immunoblotting and (C, D) quantification for Myhc, TGF-β, Col-I, cleaved caspase-3, Bcl-2, Bax. GAPDH was used as a loading control. Apoptosis was analyzed using FITC-annexin V and PI double staining kit, then analyzed by flow cytometry. (E) Representative flow cytometry images and (F) the quantification for FITC-annexin V-positive cells. Data are presented as mean ± S.E.M. n = 3 independent experiments; *p < 0.05, *versus* PA.

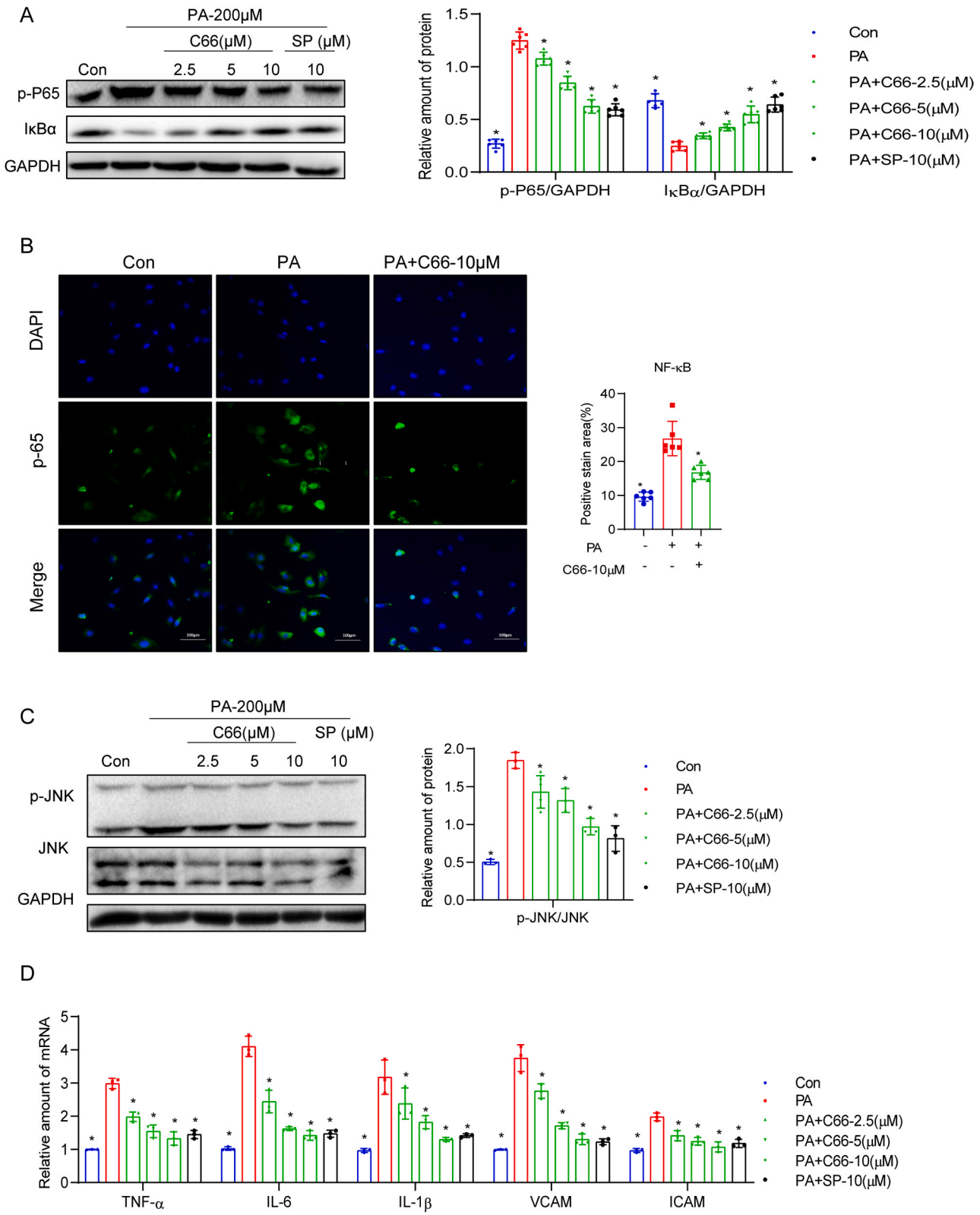

Fig. 5. C66 inhibits PA-induced NF-κB and JNK activation, and C66 treatment or JNK inhibition prevents the expression of inflammatory genes in H9c2 cells. H9c2 cells were pretreated with 2.5, 5, 10 μM of C66 or 10 μM of JNK inhibitor SP600125 for 2 h followed by exposure to PA (200 μM) for an additional 2 h, and then immunoblotting and immunofluorescence was performed. (A) Immunoblot and quantification for p-P65 and IκBα. (B) Immunofluorescence detection and quantification of p65 (green) and its translocation to the nucleus. (C) Immunoblot and quantification for p-JNK and JNK. (D) H9c2 cells were pretreated with 2.5, 5, 10 μM of C66 or 10 μM of JNK inhibitor SP600125 for 2 h followed by exposure to PA (200 μM) for an additional 12 h, and then RNAs were collected to perform qPCR for TNF-α, IL-6, IL-1β, VACM and ICAM. Data normalized to β-actin gene. Data are presented as mean ± S.E.M. n = 3 independent experiments; *$p < 0.05$, *vs* PA. (For interpretation of the references to color in this figure legend, the reader is referred to the web version of this article.)

expression, TNFα expression and apoptosis in the heart *in vivo* and PA-treated cardiomyocytes *in vitro*. However, C66 treatment significantly reduced all these measured indices, which is in line with our previous report on diabetic cardiomyopathy [12]. The JNK inhibitor, like C66, also inhibited the expression of pro-fibrotic genes in PA-treated cardiomyocytes. Given that inhibition of JNK by a specific inhibitor SP600125 provided a similar outcome as inhibition by C66, indicate that the cardioprotective effect of C66 is attributed to its ability to directly interact and inhibit the JNK pathway to protect against obesity-induced cardiac dysfunction.

Although we have previously confirmed the direct binding and inhibition of C66 on JNK protein [12], we acknowledge that C66 may have other potential targets which are also involved in its pharmacological effects. In addition to NF-κB and Bcl-2/Bax, JNK inhibition by C66 may affect other signaling pathways, including PI3K/AKT, to contribute to its cardioprotective effects. Such aspects should be further investigated in the future. A schematic diagram depicting possible mechanisms involved in the beneficial effects of C66 in diabetic cardiomyopathy has been previously concluded [37]. Anyway, using C66 and a commercial JNK inhibitor SP600125 in this study, we provided a deeper understanding of the regulatory role of JNK in obesity-induced cardiac inflammation and apoptosis, indicating that JNK inhibition may be a feasible strategy for treating obesity-associated cardiomyopathy.

We have previously reported an inhibitory effect of C66 on diabetes-related hypertriglyceridemia and lipid deregulation [12]. Accordingly, C66-treatment protected mice against obesity-related hypertriglyceridemia and lipid deregulation, which may or may not be dependent on the effects of C66 on JNK signaling. These findings warrant further investigations and suggest the therapeutic application of C66 in hypertriglyceridemia and lipid deregulation-associated CVDs. Curcumin analog C66 is also an anti-oxidant and scavenges reactive oxygen species (ROS) products [38], and can prevent ER stress-induced apoptosis [38], however, the effect of C66 on obesity-induced ROS and ER-stress in the heart and their contribution towards cardiac dysfunction or C66-mediated cardio-protection remains to be elucidated. There is still the need to further delineate the exact contribution of JNK and the detailed mechanisms of C66 action.

In summary, our data demonstrated that C66 provides significant protection against obesity-induced cardiac dysfunction, mainly by inhibiting JNK activation and JNK-mediated inflammation. Nevertheless, our new and exciting data clearly indicate that inhibition of JNK is sufficient to provide significant protection against obesity-induced cardiac dysfunction, supporting the potential clinical applications of JNK inhibition and warranting further investigations in this direction.

Funding

This study was supported by the National Key Research Project (2019ZX09301148 to Y.W.), National Natural Science Foundation of China (82000793 to W.L., 21961142009 to G.L., and 81770799 to X.G.), Thailand Research Fund Grant (DBG6280006 to N.C.), and Zhejiang Provincial Key Scientific Project (2018C03068 to J.F. and 2021C03041 to G.L.).

CRediT authorship contribution statement

This work was carried out in collaboration among all authors. Guang Liang, Wu Luo, Nipon Chattipakorn, and Yi Wang contributed to the literature search and study design. Guang Liang, Lin Ye, and Wu Luo participated in the drafting of the article. Lin Ye, Minxiu Wang, Leiming Jin, Zaishou Zhuang, Daona Yang, and Leiming Jin carried out the experiments. Aleksandr V. Samorodov and Valentin N. Pavlov revised the manuscript. Jianpeng Feng and Xinfu Guan contributed to data collection and analysis. All authors have read and approved the final manuscript. All authors contributed to data analysis, drafting or revising the article, agreed on the journal to which the article will be submitted, gave final approval of the version to be published, and agreed to be accountable for all aspects of the work.

Consent for publication

Not applicable.

Conflict of interest statement

All the authors declare that they have no conflict of interest.

Appendix A. Supporting information

Supplementary data associated with this article can be found in the online version at doi:10.1016/j.biopha.2021.112121.

References

[1] S. Wang, J. Ren, Obesity paradox in aging: from prevalence to pathophysiology, Prog. Cardiovasc. Dis. 61 (2) (2018) 182–189.
[2] H.C. Nguyen, M. Qadura, K.K. Singh, Role of the fatty acid binding proteins in cardiovascular diseases: a systematic review, J. Clin. Med. 9 (11) (2020).
[3] M. Stepien, A. Stepien, R.N. Wlazel, M. Paradowski, M. Banach, J. Rysz, Obesity indices and inflammatory markers in obese non-diabetic normo- and hypertensive patients: a comparative pilot study, Lipids Health Dis. 13 (2014) 29.
[4] H. Seki, Y. Tani, M. Arita, Omega-3 PUFA derived anti-inflammatory lipid mediator resolvin E1, Prostaglandins Other Lipid Mediat. 89 (3–4) (2009) 126–130.
[5] M.S. Ellulu, I. Patimah, H. Khaza'ai, A. Rahmat, Y. Abed, Obesity and inflammation: the linking mechanism and the complications, Arch. Med Sci. 13 (4) (2017) 851–863.
[6] C.N. Lumeng, Innate immune activation in obesity, Mol. Asp. Med. 34 (1) (2013) 12–29.
[7] X. Chen, R. Das, R. Komorowski, A. Beres, M.J. Hessner, M. Mihara, W.R. Drobyski, Blockade of interleukin-6 signaling augments regulatory T-cell reconstitution and attenuates the severity of graft-versus-host disease, Blood 114 (4) (2009) 891–900.
[8] M. Sun, M. Chen, F. Dawood, U. Zurawska, J.Y. Li, T. Parker, Z. Kassiri, L. A. Kirshenbaum, M. Arnold, R. Khokha, P.P. Liu, Tumor necrosis factor-alpha mediates cardiac remodeling and ventricular dysfunction after pressure overload state, Circulation 115 (11) (2007) 1398–1407.
[9] M. Pal, M.A. Febbraio, G.I. Lancaster, The roles of c-Jun NH2-terminal kinases (JNKs) in obesity and insulin resistance, J. Physiol. 594 (2) (2016) 267–279.
[10] I. Nikolic, M. Leiva, G. Sabio, The role of stress kinases in metabolic disease, Nat. Rev. Endocrinol. 16 (12) (2020) 697–716.
[11] G. Solinas, B. Becattini, JNK at the crossroad of obesity, insulin resistance, and cell stress response, Mol. Metab. 6 (2) (2017) 174–184.
[12] Y. Pan, Y. Wang, Y. Zhao, K. Peng, W. Li, Y. Wang, J. Zhang, S. Zhou, Q. Liu, X. Li, L. Cai, G. Liang, Inhibition of JNK phosphorylation by a novel curcumin analog prevents high glucose-induced inflammation and apoptosis in cardiomyocytes and the development of diabetic cardiomyopathy, Diabetes 63 (10) (2014) 3497–3511.
[13] Y. Pan, Y. Wang, L. Cai, Y. Cai, J. Hu, C. Yu, J. Li, Z. Feng, S. Yang, X. Li, G. Liang, Inhibition of high glucose-induced inflammatory response and macrophage infiltration by a novel curcumin derivative prevents renal injury in diabetic rats, Br. J. Pharm. 166 (3) (2012) 1169–1182.
[14] G. Liang, H. Zhou, Y. Wang, E.C. Gurley, B. Feng, L. Chen, J. Xiao, S. Yang, X. Li, Inhibition of LPS-induced production of inflammatory factors in the macrophages by mono-carbonyl analogues of curcumin, J. Cell Mol. Med. 13 (9B) (2009) 3370–3379.
[15] J. Sieber, A. Weins, K. Kampe, S. Gruber, M.T. Lindenmeyer, C.D. Cohen, J. M. Orellana, P. Mundel, A.W. Jehle, Susceptibility of podocytes to palmitic acid is regulated by stearoyl-CoA desaturases 1 and 2, Am. J. Pathol. 183 (3) (2013) 735–744.
[16] J.J. Fuster, N. Ouchi, N. Gokce, K. Walsh, Obesity-induced changes in adipose tissue microenvironment and their impact on cardiovascular disease, Circ. Res. 118 (11) (2016) 1786–1807.
[17] N. Suthahar, W.C. Meijers, H.H.W. Sillje, R.A. de Boer, From inflammation to fibrosis-molecular and cellular mechanisms of myocardial tissue remodelling and perspectives on differential treatment opportunities, Curr. Heart Fail Rep. 14 (4) (2017) 235–250.
[18] M. Lodyga, E. Cambridge, H.M. Karvonen, P. Pakshir, B. Wu, S. Boo, M. Kiebalo, R. Kaarteenaho, M. Glogauer, M. Kapoor, K. Ask, B. Hinz, Cadherin-11-mediated adhesion of macrophages to myofibroblasts establishes a profibrotic niche of active TGF-β, Sci. Signal. 12 (564) (2019).
[19] S. Carlson, D. Helterline, L. Asbe, S. Dupras, E. Minami, S. Farris, A. Stempien-Otero, Cardiac macrophages adopt profibrotic/M2 phenotype in infarcted hearts: role of urokinase plasminogen activator, J. Mol. Cell Cardiol. 108 (2017) 42–49.
[20] N. Mariappan, C.M. Elks, S. Sriramula, A. Guggilam, Z. Liu, O. Borkhsenious, J. Francis, NF-kappaB-induced oxidative stress contributes to mitochondrial and cardiac dysfunction in type II diabetes, Cardiovasc. Res. 85 (3) (2010) 473–483.
[21] G. Romeo, W.H. Liu, V. Asnaghi, T.S. Kern, M. Lorenzi, Activation of nuclear factor-kappaB induced by diabetes and high glucose regulates a proapoptotic program in retinal pericytes, Diabetes 51 (7) (2002) 2241–2248.

[22] H. Hanai, K. Sugimoto, Curcumin has bright prospects for the treatment of inflammatory bowel disease, Curr. Pharm. Des. 15 (18) (2009) 2087–2094.
[23] S.R. Panicker, C.C. Kartha, Curcumin attenuates glucose-induced monocyte chemoattractant protein-1 synthesis in aortic endothelial cells by modulating the nuclear factor-kappaB pathway, Pharmacology 85 (1) (2010) 18–26.
[24] Y. Pan, X. Zhang, Y. Wang, L. Cai, L. Ren, L. Tang, J. Wang, Y. Zhao, Y. Wang, Q. Liu, X. Li, G. Liang, Targeting JNK by a new curcumin analog to inhibit NF-kB-mediated expression of cell adhesion molecules attenuates renal macrophage infiltration and injury in diabetic mice, PLoS One 8 (11) (2013) 79084.
[25] C.W. Park, J.H. Kim, J.H. Lee, Y.S. Kim, H.J. Ahn, Y.S. Shin, S.Y. Kim, E.J. Choi, Y. S. Chang, B.K. Bang, High glucose-induced intercellular adhesion molecule-1 (ICAM-1) expression through an osmotic effect in rat mesangial cells is PKC-NF-kappa B-dependent, Diabetologia 43 (12) (2000) 1544–1553.
[26] T. Kosugi, T. Nakayama, M. Heinig, L. Zhang, Y. Yuzawa, L.G. Sanchez-Lozada, C. Roncal, R.J. Johnson, T. Nakagawa, Effect of lowering uric acid on renal disease in the type 2 diabetic db/db mice, Am. J. Physiol. Ren. Physiol. 297 (2) (2009) F481–F488.
[27] J.J. Li, S.H. Lee, D.K. Kim, R. Jin, D.S. Jung, S.J. Kwak, S.H. Kim, S.H. Han, J. E. Lee, S.J. Moon, D.R. Ryu, T.H. Yoo, D.S. Han, S.W. Kang, Colchicine attenuates inflammatory cell infiltration and extracellular matrix accumulation in diabetic nephropathy, Am. J. Physiol. Ren. Physiol. 297 (1) (2009) F200–F209.
[28] M. Watanabe, H. Nakashima, S. Mochizuki, Y. Abe, A. Ishimura, K. Ito, T. Fukushima, K. Miyake, S. Ogahara, T. Saito, Amelioration of diabetic nephropathy in OLETF rats by prostaglandin I(2) analog, beraprost sodium, Am. J. Nephrol. 30 (1) (2009) 1–11.
[29] S. Papa, F. Zazzeroni, C.G. Pham, C. Bubici, G. Franzoso, Linking JNK signaling to NF-kappaB: a key to survival, J. Cell Sci. 117 (Pt 22) (2004) 5197–5208.
[30] H. Liu, C.R. Lo, M.J. Czaja, NF-kappaB inhibition sensitizes hepatocytes to TNF-induced apoptosis through a sustained activation of JNK and c-Jun, Hepatology 35 (4) (2002) 772–778.
[31] F.M. Ho, S.H. Liu, C.S. Liau, P.J. Huang, S.Y. Lin-Shiau, High glucose-induced apoptosis in human endothelial cells is mediated by sequential activations of c-Jun NH(2)-terminal kinase and caspase-3, Circulation 101 (22) (2000) 2618–2624.
[32] D. Westermann, S. Van Linthout, S. Dhayat, N. Dhayat, A. Schmidt, M. Noutsias, X. Y. Song, F. Spillmann, A. Riad, H.P. Schultheiss, C. Tschope, Tumor necrosis factor-alpha antagonism protects from myocardial inflammation and fibrosis in experimental diabetic cardiomyopathy, Basic Res. Cardiol. 102 (6) (2007) 500–507.
[33] M. Vaishnav, M. MacFarlane, M. Dickens, Disassembly of the JIP1/JNK molecular scaffold by caspase-3-mediated cleavage of JIP1 during apoptosis, Exp. Cell Res. 317 (7) (2011) 1028–1039.
[34] C. Hull, G. McLean, F. Wong, P.J. Duriez, A. Karsan, Lipopolysaccharide signals an endothelial apoptosis pathway through TNF receptor-associated factor 6-mediated activation of c-Jun NH2-terminal kinase, J. Immunol. 169 (5) (2002) 2611–2618.
[35] D. Sun, M. Shen, J. Li, W. Li, Y. Zhang, L. Zhao, Z. Zhang, Y. Yuan, H. Wang, F. Cao, Cardioprotective effects of tanshinone IIA pretreatment via kinin B2 receptor-Akt-GSK-3β dependent pathway in experimental diabetic cardiomyopathy, Cardiovasc. Diabetol. 10 (2011) 4.
[36] J.J. Ventura, P. Cogswell, R.A. Flavell, A.S. Baldwin Jr., R.J. Davis, JNK potentiates TNF-stimulated necrosis by increasing the production of cytotoxic reactive oxygen species, Genes Dev. 18 (23) (2004) 2905–2915.
[37] J. Ren, J.R. Sowers, Application of a novel curcumin analog in the management of diabetic cardiomyopathy, Diabetes 63 (10) (2014) 3166–3168.
[38] Y. Wang, S. Zhou, W. Sun, K. McClung, Y. Pan, G. Liang, Y. Tan, Y. Zhao, Q. Liu, J. Sun, L. Cai, Inhibition of JNK by novel curcumin analog C66 prevents diabetic cardiomyopathy with a preservation of cardiac metallothionein expression, Am. J. Physiol. Endocrinol. Metab. 306 (11) (2014) E1239–E1247.